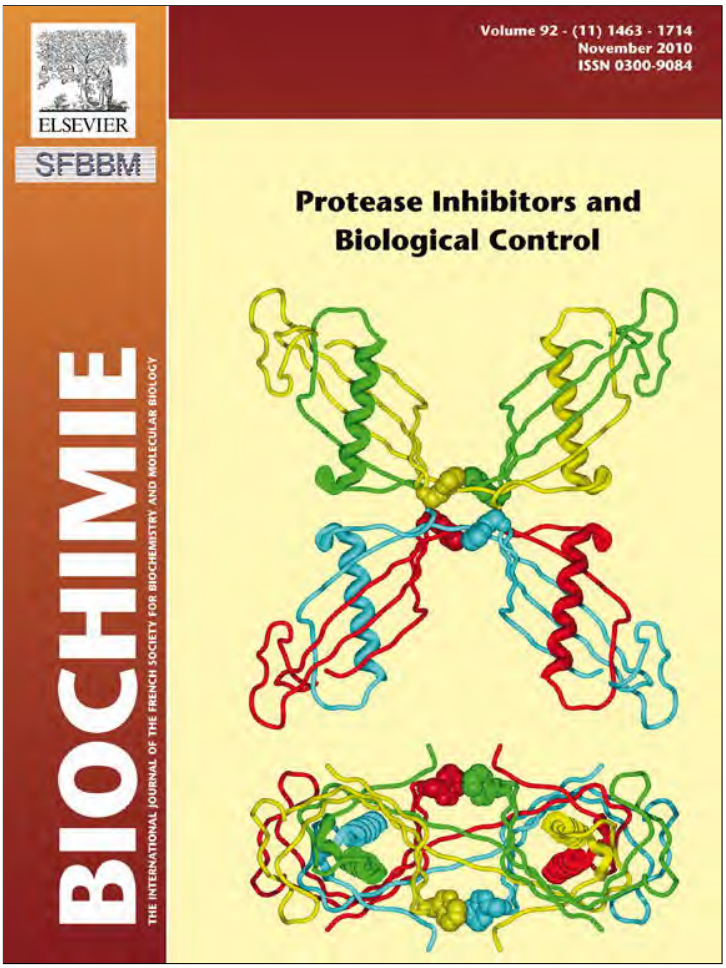

Biochimie 92 (2010) 1618–1624

Contents lists available at ScienceDirect

Biochimie

journal homepage: www.elsevier.com/locate/biochi

Research paper

Identification and pre-clinical testing of a reversible cathepsin protease inhibitor reveals anti-tumor efficacy in a pancreatic cancer model

Benelita Tina Elie [a], Vasilena Gocheva [a], Tanaya Shree [a], Stacie A. Dalrymple [b], Leslie J. Holsinger [b], Johanna A. Joyce [a,*]

[a] Cancer Biology and Genetics Program, Memorial Sloan-Kettering Cancer Center, New York, NY 10021, USA
[b] Virobay, Inc., 1490 O'Brien Drive, Menlo Park, CA 94024, USA

ARTICLE INFO

Article history:
Received 18 March 2010
Accepted 26 April 2010
Available online 4 May 2010

Keywords:
Cancer
Cysteine cathepsin
Protease
Therapy

ABSTRACT

Proteolytic activity is required for several key processes in cancer development and progression, including tumor growth, invasion and metastasis. Accordingly, high levels of protease expression and activity have been found to correlate with malignant progression and poor patient prognosis in a wide variety of human cancers. Members of the papain family of cysteine cathepsins are among the protease classes that have been functionally implicated in cancer. Therefore, the discovery of effective cathepsin inhibitors has considerable potential for anti-cancer therapy. In this study we describe the identification of a novel, reversible cathepsin inhibitor, VBY-825, which has high potency against cathepsins B, L, S and V. VBY-825 was tested in a pre-clinical model of pancreatic islet cancer and found to significantly decrease tumor burden and tumor number. Thus, the identification of VBY-825 as a new and effective anti-tumor drug encourages the therapeutic application of cathepsin inhibitors in cancer.

1. Introduction

During the development and progression of malignant tumors there are several key stages that require the concerted action of proteases. Proteolytic activity is known to be important for angiogenesis, invasion and metastasis; processes that require degradation of the basement membrane (BM) and extracellular matrix (ECM) for blood vessel formation and the dissemination of cancer cells from the primary tumor mass [1,2]. The recognition that proteolysis is required for multiple stages in the development of malignant cancers emphasizes the therapeutic importance of identifying the key tumor-promoting proteases and developing successful strategies to inhibit their functions [3–5].

One of the protease families that have been implicated in tumor development is the papain family of cysteine cathepsins. There are 11 human cysteine cathepsin proteases (B, C, F, H, K, L, O, S, L2/V, W, X/Z) that share a conserved active site formed by cysteine and histidine residues [6]. Cysteine cathepsins are produced at high levels in a wide variety of human cancers, including lung, breast, ovarian, brain, pancreatic endocrine, head and neck cancer and melanoma, and their elevated expression and/or activity typically correlates with poor patient prognosis (reviewed in Ref. [7]). Increased cathepsin expression and activity have also been reported in several transgenic mouse models of cancer [8–10], enabling pharmacological and genetic studies that have identified important tumor-promoting roles for certain cathepsins. For example, we found that treatment of the RIP1-Tag2 (RT2) transgenic model of pancreatic islet cancer with a pan-cathepsin irreversible, covalent inhibitor, JPM-OEt, significantly reduced tumor growth, angiogenesis and invasion, alone or in combination with chemotherapy [8,11]. Moreover, using gene knockouts for several cathepsin family members, we and others have identified tumor-promoting functions for cathepsins B, H, L [12,13] and S [12,14] in this model. Cathepsins B and Z were also shown to promote mammary tumorigenesis in the MMTV-PyMT model of breast cancer [10,15]. Thus, there is an emerging body of evidence supporting the consideration of cathepsins as an anti-cancer drug target (reviewed in Refs. [4,16,17]).

Several different approaches have been used to block cathepsin activity *in vivo* including small molecule inhibitors, antibodies, and increased production of endogenous inhibitors (the cystatins and stefins) (reviewed in Ref. [4]). Distinct classes of chemical structures have been developed for cysteine cathepsin inhibition, and are reviewed in detail elsewhere [6,18–20]. The major types of small molecule cathepsin inhibitors that have been tested in animal models and/or clinical trials are nitriles, vinyl sulfones and epoxysuccinyl-based compounds, either broad-spectrum or selective for individual family members [8,11,21–24]. All of these inhibitors are

* Corresponding author.
E-mail address: joycej@mskcc.org (J.A. Joyce).

0300-9084/$ – see front matter © 2010 Elsevier Masson SAS. All rights reserved.
doi:10.1016/j.biochi.2010.04.023

directed to the active site and, depending on their mechanism of action, are further classified into covalent or non-covalent binders, and reversible or irreversible inhibitors. The discovery of cathepsin inhibitors has largely followed the traditional process used for other protease families; large libraries of natural products or synthetic compounds were screened for inhibition of cathepsin activity *in vitro*, these initial screens were then followed by smaller, focused screens and/or subsequent modification of the chemical structure to achieve optimal inhibition of the target.

While we previously found that the epoxide-based inhibitor, JPM-OEt, which binds covalently and irreversibly to cathepsins, significantly impaired RT2 tumor progression [8], some concerns have been raised in the pharmaceutical industry over the potential for immune side effects in association with long-term use of irreversible inhibitors. We therefore investigated whether reversible cathepsin inhibitors might have similar anti-tumor efficacy to JPM-OEt in pre-clinical trials. The reversible covalent inhibitor VBY-825 was identified from an X-ray crystal structure-based drug design program and found to have potent inhibitory effects on several cathepsin family members, in addition to sustained bioavailability *in vivo*. We thus tested VBY-825 on established tumors in an intervention trial in the RT2 model and found that this inhibitor significantly reduced tumor number and tumor growth.

2. Materials and methods

2.1. Identification of the cathepsin inhibitor VBY-825

VBY-825 was identified as part of an extensive structure-based drug discovery program originally performed at Celera Genomics in South San Francisco, CA, USA and now Virobay Inc, Menlo Park, CA. The program was focused on the design of inhibitors highly selective for cysteine cathepsins and specifically for cathepsin S. This program developed inhibitors with exquisite selectivity for cathepsins over other cysteine and serine proteases. Many of these inhibitors had specific selectivity for cathepsin S, with a high level of potency while achieving good pharmacokinetic properties (for review, see [25]). In addition, a series of compounds was developed with broad activity against multiple cathepsins, including the ketoamide VBY-825, capable of forming a reversible covalent hemiothioketal linkage with the active site of a number of cysteine cathepsins. The detailed chemical synthesis of this compound can be found in the patent WO 2006/102 243 and the chemical structure is shown in Fig. 1A.

2.2. In vitro potency determination

The *in vitro* inhibition capacity of VBY-825 was assayed with purified cathepsins B, F, K, L, S, and V. All enzymes used in the study, with the exception of cathepsin B, were produced at Virobay Inc. using in-house expression systems. Cathepsin B from human liver was purchased from Athens Research and Technology (Athens, GA, USA). Cathepsin proteins in reaction buffer, optimized for each enzyme, were mixed with the VBY-825 inhibitor at various concentrations and allowed to incubate for 30 min at ambient temperature, after which peptide substrates specific for each cathepsin were added to initiate the reaction. Assay conditions were as follows: cathepsin B, 50 mM MES pH 6.0, 2.5 mM DTT, 2.5 mM EDTA, 0.001% Tween-20, and 10% DMSO; cathepsin F, 50 mM MES pH 6.5, 2.5 mM DTT, 2.5 mM EDTA, 100 mM NaCl, 0.01% BSA, and 10% DMSO; cathepsin K, 50 mM MES pH 6.5, 2.5 mM DTT, 2.5 mM EDTA, and 10% DMSO; cathepsin L, 50 mM MES pH 5.5, 2.5 mM DTT, 2.5 mM EDTA, 0.01% BSA, and 10% DMSO; cathepsin L2/V, 50 mM MES pH 6.5, 2.5 mM DTT, 2.5 mM EDTA, 100 mM NaCl, 0.01% BSA, and 10% DMSO; cathepsin S, 50 mM MES pH 6.5, 2.5 mM DTT, 2.5 mM EDTA, 100 mM NaCl, 0.001% BSA, and 10% DMSO. Hydrolysis of specific substrates yields the fluorescent product 7-amino-4-methylcoumarin, which was detected using an FMAX 96-well plate reader. The increase in fluorescence was measured during a 5 min assay duration that was run under conditions such that substrate concentration was close to the K_M value. Substrates were purchased from Bachem, Torrance, CA and were as follows: cathepsin B (Boc-Leu-Lys-Arg-AMC); cathepsin F (Z-Phe-Arg-AMC); cathepsin K, L, V (Z-Phe-Arg-AMC); cathepsin S (Z-Val-Val-Arg-AMC).

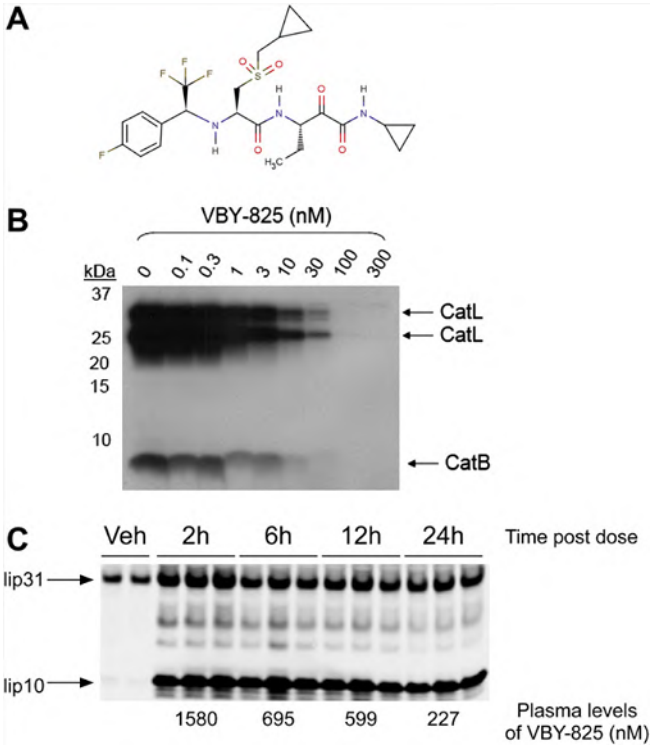

Fig. 1. Identification and characterization of the selective cathepsin inhibitor VBY-825. (A) Chemical structure of VBY-825. (B) Analysis of VBY-825 inhibition on cathepsin B and L activity in intact HUVECs using a radioiodinated diazomethylketone-Tyr-Ala (^{125}I-DMK) activity-based probe. Cells were incubated with varying concentrations of VBY-825 followed by a short incubation with ^{125}I-DMK, and IC_{50} values of inhibition were determined. The IC_{50} values for inhibition of the two heavy chain isoforms of cellular cathepsin L were 0.5 nM and 3.3 nM. The IC_{50} value for inhibition of cathepsin B was 4.3 nM (C) lip10 accumulation demonstrating cathepsin S inhibition in spleen, and VBY-825 plasma concentrations in mice following 3 days of subcutaneous QD administration of VBY-825 at 10 mg/kg. Times indicated are timepoints following the third dose, and plasma levels indicate the average plasma concentration of VBY-825 (nM) in plasma from three mice at each time point. Veh = D5W vehicle.

2.3. Cellular potency determination with cathepsin activity-based probe

An iodinated activity-based probe Diazomethylketone-Tyr-Ala ^{125}I (^{125}I-DMK) was synthesized at PerkinElmer (Shelton, CT). This is an irreversible probe that binds to cysteine cathepsins and its level of binding in cells is proportional to the activity of these proteases. The procedure was modified from that originally described in Falgueyret et al. [26]. Human umbilical venous endothelial cells (HUVEC) were treated with varying concentrations of VBY-825 for 4 h and subsequently incubated for 1 h with the radiolabeled activity-based probe. Media used throughout the experiment was serum-free and supplemented with 2% Nutridoma-HU (Boehringer Mannheim, Indianapolis, IN). 2 μCi of

iodinated probe with a specific activity of 2000 Ci/mmol was used. After incubation with the probe, cell monolayers were washed with PBS and solubilized with M-PER lysis buffer (Pierce/Thermo Scientific, Rockford, IL). Clarified lysates were boiled for 5 min and analyzed under reducing conditions with SDS-PAGE. Gels were fixed for 45 min in 10% methanol/10% acetic acid prior to drying. Binding of the probe to cathepsins B and L was assessed by SDS-PAGE followed by autoradiography. Images were scanned, and IC_{50} values of inhibition were extrapolated from the dose-response curves using GraphPad Prism.

2.4. Invariant chain processing analysis in spleen and bio-analytic methods

Spleen tissue was snap frozen on dry ice at various times following administration of VBY-825. Spleen tissue was homogenized, lysates produced, and equal amounts of total protein assessed with SDS-PAGE with 4–20% Bis Tris Criterion XT gels. Invariant chain intermediates were visualized by western blot using an antibody to mouse CD74/invariant chain (Becton Dickinson, NJ) and visualized with an HRP-conjugated donkey anti-rat secondary antibody (Jackson Immunoresearch, West Grove, PA). Bio-analytical determination of VBY-825 plasma concentrations was performed using liquid chromatography with tandem mass spectrometric detection. Samples were analyzed using a Thermo Scientific AQUASIL C18 column followed by spectrometric detection using a Sciex API 4000.

2.5. Experimental animals and trial design

The generation of RIP1-Tag2 (RT2) mice as a model of pancreatic islet cell carcinogenesis has been reported previously [27]. RT2 mice were maintained in accordance with institutional guidelines at MSKCC governing the care of laboratory animals. All RT2 mice on trial received 50% sucrose-adjusted diet (Harlan Teklad, Madison, WI) and 5% sugar water to relieve hypoglycemia induced by the insulin-secreting tumors. The mice were weighed twice per week. VBY-825 was administered in 5% dextrose solution (D5W) (Baxter I.V. Solutions, West Chester, PA) once daily by subcutaneous injection at a dose of 10 mg/kg/day. A separate cohort of mice were treated with the D5W vehicle control, administered once daily by subcutaneous injection. RT2 mice were treated in an intervention trial from 10 to 13.5 weeks of age, and sacrificed at 13.5 weeks. Two independent trials were performed on different cohorts of sex-matched mice, with the following numbers per treatment group: D5W $n = 18$ mice total ($n = 12$ and $n = 6$ from two separate trials); VBY-825 $n = 21$ mice ($n = 12$ and $n = 9$ from two separate trials).

2.6. Tumor burden analysis

Mice were anesthetized and underwent heart perfusion using 10 ml PBS followed by 10 ml 10% zinc-buffered formalin (Medical Chemical Corp., Torrance, CA). The pancreas and spleen of the mice were dissected and macroscopic tumors ($\geq 1 \times 1$ mm) were excised and measured. Tumor volume was calculated using the formula $V = a^*b^2*pi/6$ where a and b equal the longer and shorter diameter of the tumor, respectively. The volumes of all tumors from each mouse were added to give the cumulative tumor burden per animal.

2.7. Tissue preparation and immunohistochemistry

Tissues were prepared as previously described for frozen and paraffin embedding [28]. For the angiogenesis analysis, the vasculature was visualized with a rat anti-mouse CD31 antibody (BD Pharmingen, San Diego, CA) and a donkey-anti-rat Alexa 568 secondary antibody for subsequent detection (Molecular Probes, Eugene, OR). Vessel leakiness was assessed following intravenous injection of 100 μl of lysine fixable, Texas Red conjugated dextran (70 kDa, Molecular Probes, Eugene, OR). Vessel functionality was assessed by FITC-lectin (Vector Labs, Burlingame, CA) perfusion and visualization as previously described [29]. Apoptotic cells were visualized using a rabbit anti-mouse cleaved caspase 3 antibody (Cell Signaling Technology, Beverly, MA) and a goat anti-rabbit Alexa 568 secondary antibody (Molecular Probes, Eugene, OR). DAPI (Invitrogen, Eugene OR) was used to visualize the nuclei and the slides were mounted in ProLong Gold Mounting Medium (Invitrogen, Eugene, OR). Proliferating cells were identified using a rabbit anti-mouse Ki67 antibody (Vector Labs, Burlingame, CA) and SIGMA*FAST* 3,3′-Diaminobenzidine (DAB) (Sigma Aldrich, St. Louis, MO) detection; nuclei were counterstained with hematoxylin (Sigma Aldrich, St. Louis, MO). For the invasion analysis, paraffin sections were stained with hematoxylin and eosin Y (H&E) solutions (Sigma Aldrich, St. Louis, MO) and grading was performed as previously described [28].

2.8. Analysis of cell proliferation, apoptosis, tumor vasculature and tumor invasion

For all histological analyses, VBY-825 treated tumors were compared to vehicle controls at the 13.5 week-old endpoint of the intervention trial. Tumors were analyzed from at least 5 mice per treatment group with the exception of the invasion analysis, which was performed on 15 mice per group, and all tumors per mouse were analyzed. Images were acquired on a Carl Zeiss AxioImager Z1 equipped with a high-precision scanning stage using TissueFAXS image acquisition software and the TissueStitching function (TissueGnostics, Vienna, Austria). Cell proliferation was quantified using HistoQuest analysis software (TissueGnostics, Vienna, Austria) and was calculated as the percentage of Ki67 positive cells over the total number of cells per tumor. Apoptosis was quantified by counting the number of cleaved caspase 3-positive cells per tumor using TissueQuest analysis software (TissueGnostics, Vienna, Austria). Vessel area, as determined by CD31 staining and dextran-covered area, was quantified using Metamorph imaging software (Molecular Devices, Sunnyvale, CA). For all analyses, tumor images were analyzed in a genotype-blinded manner and subsequently decoded. For analysis of tumor invasion, tissue sections were stained by H&E and graded as previously described [28] in a blinded manner by two independent investigators (BTE and JAJ).

2.9. Statistical analysis

For analysis of tumor burden, cell proliferation, apoptosis and vessel area, means and standard errors were calculated per mouse from each treatment group using the unpaired Student's t-test, and were considered statistically significant if $P < 0.05$. Statistical comparison of tumor grades in the invasion analysis was performed using a cumulative logit model [30] with generalized estimating equations to correct for correlations within individual mice.

3. Results

3.1. Identification and chemical structure of the cathepsin inhibitor VBY-825

An extensive X-ray crystal structure-based drug design program was performed to identify cathepsin-selective inhibitors with different inhibitory profiles for various cathepsins primarily cathepsin S, which was targeted for autoimmunity therapy. In

addition to cathepsin S-selective inhibitors, this program led to the discovery of the inhibitor VBY-825, which binds to a spectrum of cathepsins with a fully reversible covalent hemiothioketal linkage to the active site cysteine and via structural elements binding at the S1, S2 and S3 binding pockets of the enzymes, based on the cathepsin S structure determination by McGrath et al [31]. The chemical structure of VBY-825 is shown in Fig. 1A. This inhibitor has good metabolic stability (93% remaining at 60 min in human liver microsomes; 82% remaining at 60 min in human plasma) and acceptable kinetic solubility (223 μM in phosphate buffered saline pH 7.4) (data not shown).

3.2. Analysis of the potency of enzyme inhibition by VBY-825

VBY-825 was screened against six purified human cathepsins to determine the potency against these enzymes. $K_i(app)$ values were obtained and are as follows: cathepsin S = 130 pM, cathepsin L = 250 pM, cathepsin V = 250 pM, cathepsin B = 330 pM, humanized-rabbit cathepsin K = 2.3 nM, cathepsin F = 4.7 nM. The potency ($K_i(app)$) values were also determined against four species orthologues of cathepsin S and are as follows: mouse = 40 pM, monkey = 60 pM, dog = 250 pM, rat = 770 pM. These data indicate that VBY-825 is a potent inhibitor of the assayed cathepsins and its potency against at least one cathepsin, cathepsin S, extends across species relevant for pharmacology studies, specifically mouse.

In addition to these *in vitro* enzyme potency assays, the activity of VBY-825 against cathepsins B and L was also determined in intact cells using an activity-based probe. Studies were performed in human umbilical vein endothelial cells (HUVEC) as this cell line expresses both cathepsins B and L. Briefly, cells were incubated with varying concentrations of VBY-825 followed by a short incubation with the radioiodinated diazomethylketone-Tyr-Ala (^{125}I-DMK) activity-based probe. This probe binds irreversibly to cysteine proteases including cathepsins B and L. It was used in a whole-cell enzyme occupancy assay to determine cellular potency of VBY-825 as a quantitative marker of protease activity based on the protocol described previously [26]. Data are shown in Fig. 1B, and IC_{50} values of inhibition were determined. The IC_{50} values for inhibition of the two heavy chain isoforms of cellular cathepsin L were 0.5 nM and 3.3 nM. The IC_{50} value for inhibition of cathepsin B was 4.3 nM. These studies were also performed in the mouse macrophage-like cell line J774.A1 and similar potencies were obtained (data not shown). These results are consistent with the high potency for VBY-825 against purified cathepsin enzymes and demonstrate that VBY-825 is highly effective in inhibiting these enzymes in cells.

3.3. Pharmacokinetics and pharmacodynamics of VBY-825 in mice

C57BL/6 mice were treated daily for three days with either VBY-825 (10 mg/kg/day) or a vehicle control (D5W). Plasma concentrations of VBY-825 were obtained at 2, 6, 12, and 24 h following the final dose. Bio-analytical determination of plasma concentrations was performed using liquid chromatography (LC) with tandem mass spectrometric detection (MS/MS). Plasma levels exceeded 1.5 μM at 2 h after dosing and remained above 200 nM for the full 24 h after dosing (Fig. 1C). The invariant chain processing intermediate Iip10, a substrate of cathepsin S in antigen presenting cells, is a pharmacodynamic biomarker of cathepsin S inhibition. Its accumulation indicates complete inhibition of cathepsin S in antigen presenting cells, which require cathepsin S for Iip10 proteolysis [32–34]. Iip10 accumulation was assessed in the spleen of three VBY-825 dosed animals at each time point in this analysis compared to vehicle-treated mice. Iip10 was detected in all VBY-825 treated mice at all time points, reflecting the complete inhibition of cathepsin S in spleen tissue during the duration of dosing (Fig. 1C). These pharmacokinetic studies demonstrate that the 10 mg/kg/day dose of VBY-825 achieves a trough plasma concentration >200 nM, which is well above that required for full inhibition of the intracellular activity of cathepsins B, F, K, L, S and V in both mouse and human cell lines (Fig. 1B and data not shown).

3.4. VBY-825 reduces tumor growth and number in a RT2 intervention trial

While these experiments demonstrated the inhibitory effects of VBY-825 on cathepsins in biochemical and cell-based assays, we wanted to know whether VBY-825 had similar effects *in vivo*. We used the well-characterized RIP1-Tag2 (RT2) mouse model of pancreatic neuroendocrine cancer, which has been very informative as a pre-clinical platform for evaluating novel drug treatments, including different anti-angiogenic agents, protease inhibitors and chemotherapy (reviewed in [35]). Tumor development in RT2 mice is highly reproducible, and progresses through defined sequential stages including hyperplastic/dysplastic islets, angiogenic islets, and progressive grades of carcinoma [27]. As such, RT2 mice have been used in stage-specific trials to investigate the effects of different inhibitors on reducing angiogenic switching and tumor growth, and inducing tumor regression. In the present study we chose to use an "intervention trial" design with treatment between 10 and 13.5 weeks of age to focus our investigation on rapidly growing tumors. This was also the time window in which we had previously found the most dramatic reduction in tumor growth with an irreversible cathepsin inhibitor, JPM-OEt, in a similar trial design [8], and thus the most logical to use for comparison with a reversible inhibitor in the current study.

Two different cohorts of RT2 mice were treated daily with either VBY-825 (10 mg/kg/day) or the vehicle control (D5W) beginning at 10 weeks of age. VBY-825 was very well tolerated, with no observed weight loss or evidence of any side effects. Mice were sacrificed at the trial endpoint of 13.5 weeks of age, the pancreas was removed and islet cell tumors dissected from the pancreas. Tumors were counted, and the individual and cumulative tumor volumes calculated for each mouse. Lesions in RT2 mice continue to progress to carcinomas during the timeframe of the intervention trial performed in the current study. In the control D5W-treated group the mean tumor number at the 13.5 week trial endpoint was 8.7 tumors. We found that treatment with VBY-825 significantly reduced the number of tumors by 33% to a mean value of 5.8 (Fig. 2A, $P < 0.05$). There was also a substantial 52% decrease in cumulative tumor volume following VBY-825 treatment (mean = 20.59 mm^3) compared to the vehicle control group (mean = 42.97 mm^3) (Fig. 2B, $P < 0.01$).

3.5. Effects of VBY-825 on the balance between cell proliferation and apoptosis in RT2 tumors

Given the significant decrease in tumor growth in VBY-825 treated RT2 mice, we next sought to identify the cellular mechanisms underlying this reduction. We first examined cell proliferation in RT2 tumors using the proliferation marker Ki67. The mean percentage of proliferating cells in individual tumors from the vehicle control group was 8.2%, which was reduced to 6.1% in tumors from VBY-825 treated mice (Fig. 3A, $n = 5$ mice per group; 25% decrease). Tumor growth can also be affected by alterations in cell death, and so we next compared apoptotic rates in the two groups using an antibody that detects the cleaved, active form of caspase 3. We found that the percentage of apoptotic cells in individual tumors was increased from a mean of 0.77% in the control group to 1.10% in the VBY-825 group (Fig. 3B, $n = 5$ mice per

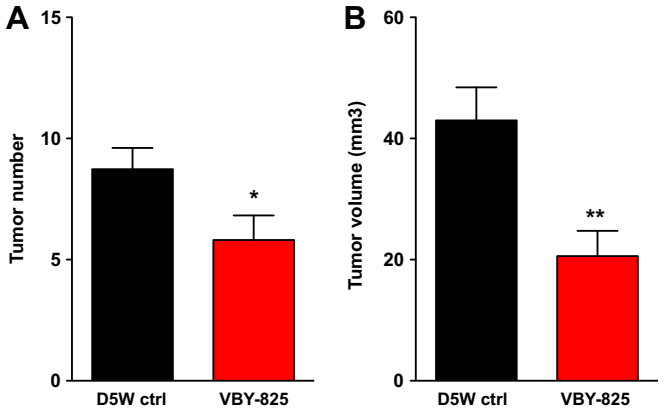

Fig. 2. VBY-825 treatment reduces tumor incidence and tumor growth in a RT2 intervention trial. (A) Tumor number was decreased by 33% in VBY-825 treated RT2 mice compared to the D5W vehicle control-treated cohort, $^{*}P < 0.05$. Mice were treated with D5W or VBY-825 (10 mg/kg/day) once daily by subcutaneous injection from 10 to 13.5 weeks of age. D5W: $n = 18$ mice, VBY-825: $n = 21$ mice. (B) The cumulative tumor volume at the 13.5 week trial endpoint was decreased by 52% in VBY-825 treated RT2 mice compared to the D5W vehicle control-treated group, $^{**}P < 0.01$.

group; 42% increase). Although these effects did not reach statistical significance, it is possible that changes in the overall balance between cell proliferation and apoptosis may contribute to the decreased tumor burden observed in VBY-825 treated animals.

3.6. Analysis of the effects of VBY-825 treatment on RT2 tumor invasion and vascularization

We have previously shown that inhibition or deletion of cathepsin proteases in RT2 mice leads to a significant reduction in tumor invasion and angiogenesis [8,11,12,14,36], and thus sought to determine whether reversible inhibition of selective cathepsins affected these processes. Tumor invasion was scored as previously described [28] for all tumors detectable in H&E stained sections from the two treatment groups ($n = 15$ mice per group). Tumors were categorized as encapsulated, microinvasive, or invasive. As shown in Fig. 4A, the majority of tumors in the vehicle control animals were either microinvasive or frankly invasive. VBY-825 treatment resulted in a modest shift in the distribution of tumors to less invasive types, but this did not reach statistical significance.

Another tumorigenic process that requires proteolytic degradation is angiogenesis, in which important roles have been identified for cathepsins [8,11–14,36–39], and so we asked whether tumor vascularization was altered in VBY-825 treated tumors. Vessels were detected using the endothelial cell-specific antibody CD31, and vessel coverage over tumor area was assessed. We found no significant difference in the area covered by CD31 + cells in the VBY-825 treated group compared to vehicle controls (Fig. 4B). We also asked whether vessel functionality was affected by injecting either FITC-conjugated lectin, which binds to the lumen of functional blood vessels, or Texas Red-conjugated dextran, which diffuses more readily from leaky blood vessels. We analyzed the distribution of both molecules within the tumors and found no difference between the VBY-825 treated and vehicle control groups (Fig. 4C and data not shown), indicating that vessel density and functionality were not affected following VBY-825 treatment.

4. Discussion

In this study we report the identification, characterization and *in vivo* testing of a novel reversible cathepsin inhibitor, VBY-825, in

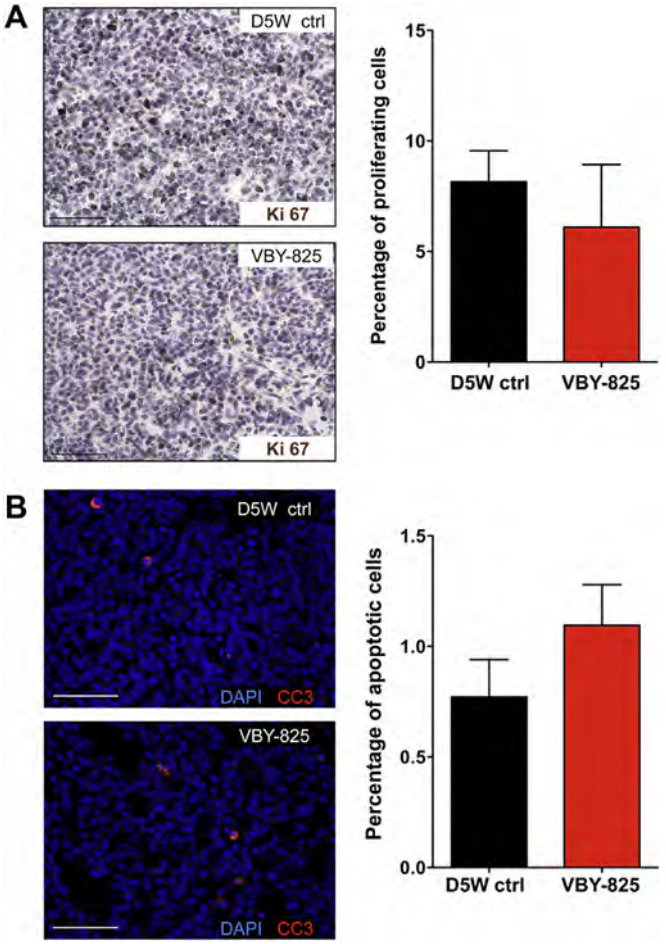

Fig. 3. Effects of VBY-825 treatment on the balance between cell proliferation and apoptosis in RT2 tumors. (A) Proliferating cells were detected by Ki67 staining (brown) and representative images are shown for D5W-treated tumors (upper panel) and VBY-825 treated tumors (lower panel) at the 13.5 week trial endpoint. Scale bar = 50 μm. Graph on the right shows the percentage of proliferating cells (Ki67 positive) over the total number of hematoxylin-positive cells in the tumor. VBY-825 treatment resulted in a 25% decrease in cell proliferation. (B) Apoptotic cells were detected by cleaved caspase 3 staining (red) and representative images are shown for D5W-treated tumors (upper panel) and VBY-825 treated tumors (lower panel) at the 13.5 week trial endpoint. Scale bar = 50 μm. Graph on the right shows the percentage of apoptotic cells (cleaved caspase 3 positive) over the total number of DAPI-positive cells in the tumor. VBY-825 treatment resulted in a 42% increase in apoptosis. The means and SEM are indicated in both graphs, $n = 5$ mice per group.

a mouse model of pancreatic islet cancer. VBY-825 was identified from an extensive structure-based drug design program, and found to have high potency for inhibition of cathepsins B, L, S and V, and to a lesser extent cathepsins F and K. We have previously shown that cathepsins B, C, H, L, S and Z are upregulated during the different stages of RT2 tumorigenesis [8], whereas the remaining cathepsin family members are either not expressed, or are expressed at low levels that do not change. Thus, cathepsins B, L and S are the potential targets for inhibition by VBY-825 in this cancer model.

VBY-825 treatment in an intervention trial resulted in a significant decrease in tumor growth and tumor incidence, which was comparable to the reduction observed previously with the irreversible inhibitor JPM-OEt in a similar trial design [8]. The reduced tumor growth could potentially be explained by the trend towards a combined decrease in cell proliferation and increase in apoptosis we observed in the VBY-825 treated tumors. However, while both proliferation and cell death were somewhat perturbed following VBY-825 treatment, the effects were not as pronounced as we had

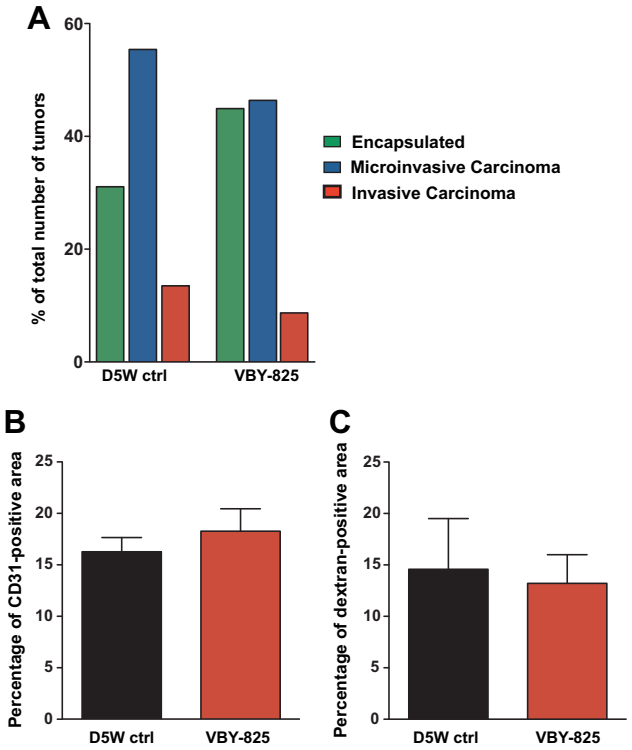

Fig. 4. VBY-825 treatment does not affect RT2 tumor invasion or angiogenesis at the 13.5 week trial endpoint. (A) Graph showing the relative proportions of encapsulated, microinvasive, and highly invasive carcinomas in 13.5 week D5W controls compared to VBY-825 treated RT2 mice. VBY-825 treatment did not significantly alter the distribution of tumor grades compared to D5W-treated mice, $n = 15$ mice per group. (B, C) The tumor vasculature was analyzed by perfusion of mice with Texas Red-dextran and by staining with an endothelial cell-specific antibody (CD31) ($n = 2–8$ mice per group). The percentage of CD31-positive blood vessels over the total tumor area (DAPI-positive) is graphed in (B), showing no difference in vessel coverage between the D5W- and VBY-825 treated tumors. The percentage of dextran-covered area over the total tumor area (DAPI-positive) is graphed in (C), showing no difference in vessel leakiness (as assessed by dextran diffusion from blood vessels) between the D5W- and VBY-825 treated tumors.

previously observed with the pan-cathepsin inhibitor JPM-OEt [8]. Similarly, we did not observe a significant difference in tumor invasion or angiogenesis in VBY-825 treated mice, in contrast to the substantial reductions in both processes that we had previously found following JPM-OEt treatment [8,11]. Thus, while both JPM-OEt and VBY-825 have a similar potency in reducing tumor growth and tumor number, there are some differences in their observed effects on the hallmark capabilities of cancer.

There are several possible explanations that may account for some of the differences between the VBY-825 and JPM-OEt inhibitors in the RT2 model. First, JPM-OEt is a pan-cathepsin inhibitor, whereas VBY-825 has a more selective inhibitory profile, with the expected targets being restricted to cathepsins B, L and S in this model. Therefore, it is possible that the remaining upregulated cathepsins (H and Z), which we know to be important for tumor angiogenesis and invasion respectively [Ref. [13], and Gocheva et al., manuscript in preparation] are not inhibited, and are sufficient to promote these tumorigenic processes when cathepsins B, L and S are inhibited by VBY-825. A second possibility is that reversible inhibition of these specific cathepsins is not as effective as irreversible inhibition in reducing tumor angiogenesis and invasion, although this is unlikely given the high plasma levels of the compound throughout the duration of dosing. Finally, it is possible that the defined timepoint of the analyses after 3.5 weeks of treatment may not reveal important but transitory effects occurring earlier in the therapeutic regimen. Analysis of these parameters at earlier timepoints following the initiation of treatment at 10 weeks could be informative in determining whether the biological effects of VBY-825 treatment are more pronounced initially. For example, it is possible there is an initial wave of increased apoptosis and decreased cell proliferation, which debulks the tumor mass, but then is attenuated by the time they are assessed histologically at the 13.5-week endpoint.

An additional consideration is the route of administration. VBY-825 was delivered via subcutaneous injection, whereas JPM-OEt was administered by intraperitoneal injection. Reinheckel and colleagues recently showed that JPM-OEt effectively inhibited cathepsin activity in the organs close to the injection site in the peritoneal cavity (pancreas, liver and kidney) but was less effective in the distally located lungs [24]. Thus examining the efficacy of intraperitoneal administration of VBY-825 in the RT2 pancreatic cancer model could be informative. Additional strategies to improve the efficacy of VBY-825 in pre-clinical trials include combining this inhibitor with other anti-cancer agents, such as chemotherapy. Indeed, we previously found that the addition of cyclophosphamide to the cathepsin inhibitor JPM-OEt significantly enhanced its anti-tumor efficacy, and increased overall survival in an RT2 regression trial [11], motivating further investigation of VBY-825 in combination with other drugs.

In conclusion, we have identified and characterized a novel, reversible and selective cathepsin inhibitor that significantly reduces tumor incidence and tumor growth in a mouse model of pancreatic islet cancer. In addition, VBY-825 treatment was non-toxic to animals over the course of this pre-clinical trial, as we have previously reported for JPM-OEt [4,8], further encouraging the potential application of cathepsin inhibitors as potent anti-cancer therapeutics. Indeed, the range of cysteine cathepsin inhibitors that have been developed and tested in animal models has significantly expanded in the past several years. In addition to the identification of selective small molecule inhibitors such as VBY-825, there have also been programs to develop antibody and peptide-based inhibitors [39–45]. Another exciting advance is the ongoing evaluation of cathepsin K-selective small molecule inhibitors in early clinical trials for patients with bone metastases [46–48]. It will thus be very interesting to establish whether the potential benefits of inhibiting cathepsins, as indicated from pre-clinical studies such as this one, will translate into a successful therapeutic strategy in the clinic.

Acknowledgements

We thank members of the Joyce lab, in particular Hao-Wei Wang, Stephanie Pyonteck, Xiaoping Chen and Keni Simpson for experimental assistance and insight. We are grateful to Elyn Riedel, MSKCC Epidemiology and Biostatistics Department, for statistical analysis and the MSKCC Molecular Cytology core facility for assistance with the Metamorph image analysis. The VBY-825 drug development program was carried out by John Link (present address Gilead Sciences, Foster City, CA) and colleagues. We acknowledge the work of Mike Roberts and Jaideep Thotasserry at Southern Research in Birmingham, Alabama for the potency studies using ^{125}I-DMK. This research was supported by funding from the National Cancer Institute (NIH R01-CA125162), NIH Cancer Center Support grant ARRA supplement (3P30CA008748-44S4), and the Geoffrey Beene Foundation (to JAJ). VG is supported by the Weill Cornell graduate program and a Geoffrey Beene fellowship, and TS is supported by the Weill Cornell-Rockefeller-Sloan Kettering Tri-Institutional MD-PhD program.

References

[1] R.G. Rowe, S.J. Weiss, Navigating ECM barriers at the invasive front: the cancer cell–stroma interface. Annu. Rev. Cell Dev. Biol. 25 (2009) 567–595.

[2] S.D. Mason, J.A. Joyce, Proteolytic Cascades in Invasion and Metastasis, Cancer Metastasis: Biologic Basis and Therapeutics. Cambridge University Press. Welsh DR, Lyden DC, Psaila B (Eds.), in press.

[3] C.M. Overall, O. Kleifeld, Tumour microenvironment - opinion: validating matrix metalloproteinases as drug targets and anti-targets for cancer therapy. Nat. Rev. Cancer 6 (2006) 227–239.

[4] C. Palermo, J.A. Joyce, Cysteine cathepsin proteases as pharmacological targets in cancer. Trends Pharmacol. Sci. 29 (2008) 22–28.

[5] S. Ulisse, E. Baldini, S. Sorrenti, M. D'Armiento, The urokinase plasminogen activator system: a target for anti-cancer therapy. Curr. Cancer Drug Targets 9 (2009) 32–71.

[6] O. Vasiljeva, T. Reinheckel, C. Peters, D. Turk, V. Turk, B. Turk, Emerging roles of cysteine cathepsins in disease and their potential as drug targets. Curr. Pharm. Des. 13 (2007) 385–401.

[7] C. Jedeszko, B.F. Sloane, Cysteine cathepsins in human cancer. Biol. Chem. 385 (2004) 1017–1027.

[8] J.A. Joyce, A. Baruch, K. Chehade, N. Meyer-Morse, E. Giraudo, F.Y. Tsai, D.C. Greenbaum, J.H. Hager, M. Bogyo, D. Hanahan, Cathepsin cysteine proteases are effectors of invasive growth and angiogenesis during multistage tumorigenesis. Cancer Cell 5 (2004) 443–453.

[9] J. Grimm, D.G. Kirsch, S.D. Windsor, C.F. Kim, P.M. Santiago, V. Ntziachristos, T. Jacks, R. Weissleder, Use of gene expression profiling to direct in vivo molecular imaging of lung cancer. Proc Natl Acad Sci U S A 102 (2005) 14404–14409.

[10] O. Vasiljeva, A. Papazoglou, A. Kruger, H. Brodoefel, M. Korovin, J. Deussing, N. Augustin, B.S. Nielsen, K. Almholt, M. Bogyo, C. Peters, T. Reinheckel, Tumor cell-derived and macrophage-derived cathepsin B promotes progression and lung metastasis of mammary cancer. Cancer Res. 66 (2006) 5242–5250.

[11] K.M. Bell-McGuinn, A.L. Garfall, M. Bogyo, D. Hanahan, J.A. Joyce, Inhibition of cysteine cathepsin protease activity enhances chemotherapy regimens by decreasing tumor growth and invasiveness in a mouse model of multistage cancer. Cancer Res. 67 (2007) 7378–7385.

[12] V. Gocheva, W. Zeng, D. Ke, D. Klimstra, T. Reinheckel, C. Peters, D. Hanahan, J.A. Joyce, Distinct roles for cysteine cathepsin genes in multistage tumorigenesis. Genes Dev. 20 (2006) 543–556.

[13] V. Gocheva, X. Chen, C. Peters, T. Reinheckel, J.A. Joyce, Deletion of cathepsin H perturbs angiogenic switching, vascularization and the growth of tumors in a mouse model of pancreatic islet cancer, Biol. Chem., in press.

[14] B. Wang, J. Sun, S. Kitamoto, M. Yang, A. Grubb, H.A. Chapman, R. Kalluri, G.P. Shi, Cathepsin S controls angiogenesis and tumor growth via matrix-derived angiogenic factors. J. Biol. Chem. 281 (2006) 6020–6029.

[15] L. Sevenich, U. Schurigt, K. Sachse, M. Gajda, F. Werner, S. Muller, O. Vasiljeva, A. Schwinde, N. Klemm, J. Deussing, C. Peters, T. Reinheckel, Synergistic antitumor effects of combined cathepsin B and cathepsin Z deficiencies on breast cancer progression and metastasis in mice. Proc Natl Acad Sci U S A 107 (2010) 2497–2502.

[16] M.M. Mohamed, B.F. Sloane, Cysteine cathepsins: multifunctional enzymes in cancer. Nat. Rev. Cancer 6 (2006) 764–775.

[17] T. Reinheckel, V. Gocheva, C. Peters, J.A. Joyce, Roles of cysteine proteases in tumor progression: analysis of cysteine cathepsin knockout mice in cancer models. in: D.R. Edwards, G. Hoer-Hansen, F. Blasi, B.F. Sloane (Eds.), The Cancer Degradome- Proteases and Cancer Biology. Springer Publishing, 2008, pp. 279–302.

[18] Y. Yasuda, J. Kaleta, D. Bromme, The role of cathepsins in osteoporosis and arthritis: rationale for the design of new therapeutics. Adv. Drug Deliv. Rev. 57 (2005) 973–993.

[19] B. Turk, Targeting proteases: successes, failures and future prospects. Nat. Rev. Drug Discov. 5 (2006) 785–799.

[20] M. Frizler, M. Stirnberg, M.T. Sisay, M. Gutschow, Development of nitrile-based peptidic inhibitors of cysteine cathepsins. Curr. Top. Med. Chem. 10 (2010) 294–322.

[21] J.P. Meara, D.H. Rich, Mechanistic studies on the inactivation of papain by epoxysuccinyl inhibitors. J. Med. Chem. 39 (1996) 3357–3366.

[22] R. Navab, J.S. Mort, P. Brodt, Inhibition of carcinoma cell invasion and liver metastases formation by the cysteine proteinase inhibitor E-64. Clin. Exp. Metastasis. 15 (1997) 121–129.

[23] A.M. Sadaghiani, S.H. Verhelst, V. Gocheva, K. Hill, E. Majerova, S. Stinson, J.A. Joyce, M. Bogyo, Design, synthesis, and evaluation of in vivo potency and selectivity of epoxysuccinyl-based inhibitors of papain-family cysteine proteases. Chem. Biol. 14 (2007) 499–511.

[24] U. Schurigt, L. Sevenich, C. Vannier, M. Gajda, A. Schwinde, F. Werner, A. Stahl, D. von Elverfeldt, A.K. Becker, M. Bogyo, C. Peters, T. Reinheckel, Trial of the cysteine cathepsin inhibitor JPM-OEt on early and advanced mammary cancer stages in the MMTV-PyMT-transgenic mouse model. Biol. Chem. 389 (2008) 1067–1074.

[25] J.O. Link, S. Zipfel, Advances in cathepsin S inhibitor design. Curr. Opin. Drug Discov. Devel. 9 (2006) 471–482.

[26] J.P. Falgueyret, W.C. Black, W. Cromlish, S. Desmarais, S. Lamontagne, C. Mellon, D. Riendeau, S. Rodan, P. Tawa, G. Wesolowski, K.E. Bass, S. Venkatraman, M.D. Percival, An activity-based probe for the determination of cysteine cathepsin protease activities in whole cells. Anal. Biochem. 335 (2004) 218–227.

[27] D. Hanahan, Heritable formation of pancreatic beta-cell tumours in transgenic mice expressing recombinant insulin/simian virus 40 oncogenes. Nature 315 (1985) 115–122.

[28] T. Lopez, D. Hanahan, Elevated levels of IGF-1 receptor convey invasive and metastatic capability in a mouse model of pancreatic islet tumorigenesis. Cancer Cell 1 (2002) 339–353.

[29] M. Inoue, J.H. Hager, N. Ferrara, H.P. Gerber, D. Hanahan, VEGF-A has a critical, nonredundant role in angiogenic switching and pancreatic beta cell carcinogenesis. Cancer Cell 1 (2002) 193–202.

[30] Mc Cullagh, Regression models for ordinal data. J.R. Statist. Soc. (1980) 109–142.

[31] M.E. McGrath, J.T. Palmer, D. Bromme, J.R. Somoza, Crystal structure of human cathepsin S. Protein Sci. 7 (1998) 1294–1302.

[32] R.J. Riese, R.N. Mitchell, J.A. Villadangos, G.P. Shi, J.T. Palmer, E.R. Karp, G.T. De Sanctis, H.L. Ploegh, H.A. Chapman, Cathepsin S activity regulates antigen presentation and immunity. J. Clin. Invest. 101 (1998) 2351–2363.

[33] T.Y. Nakagawa, W.H. Brissette, P.D. Lira, R.J. Griffiths, N. Petrushova, J. Stock, J.D. McNeish, S.E. Eastman, E.D. Howard, S.R. Clarke, E.F. Rosloniec, E.A. Elliott, A.Y. Rudensky, Impaired invariant chain degradation and antigen presentation and diminished collagen-induced arthritis in cathepsin S null mice. Immunity 10 (1999) 207–217.

[34] G.P. Shi, J.A. Villadangos, G. Dranoff, C. Small, L. Gu, K.J. Haley, R. Riese, H.L. Ploegh, H.A. Chapman, Cathepsin S required for normal MHC class II peptide loading and germinal center development. Immunity 10 (1999) 197–206.

[35] D. Ribatti, B. Nico, E. Crivellato, A.M. Roccaro, A. Vacca, The history of the angiogenic switch concept. Leukemia 21 (2007) 44–52.

[36] V. Gocheva, H.W. Wang, B.B. Gadea, T. Shree, K.E. Hunter, A.L. Garfall, T. Berman, J.A. Joyce, IL-4 induces cathepsin protease activity in tumor-associated macrophages to promote cancer growth and invasion. Genes Dev. 24 (2010) 241–255.

[37] G.P. Shi, G.K. Sukhova, M. Kuzuya, Q. Ye, J. Du, Y. Zhang, J.H. Pan, M.L. Lu, X.W. Cheng, A. Iguchi, S. Perrey, A.M. Lee, H.A. Chapman, P. Libby, Deficiency of the cysteine protease cathepsin S impairs microvessel growth. Circ. Res. 92 (2003) 493–500.

[38] S.H. Chang, K. Kanasaki, V. Gocheva, G. Blum, J. Harper, M.A. Moses, S.C. Shih, J.A. Nagy, J. Joyce, M. Bogyo, R. Kalluri, H.F. Dvorak, VEGF-A induces angiogenesis by perturbing the cathepsin-cysteine protease inhibitor balance in venules, causing basement membrane degradation and mother vessel formation. Cancer Res. 69 (2009) 4537–4544.

[39] R.E. Burden, J.A. Gormley, T.J. Jaquin, D.M. Small, D.J. Quinn, S.M. Hegarty, C. Ward, B. Walker, J.A. Johnston, S.A. Olwill, C.J. Scott, Antibody-mediated inhibition of cathepsin S blocks colorectal tumor invasion and angiogenesis. Clin. Cancer Res. 15 (2009) 6042–6051.

[40] N. Rousselet, L. Mills, D. Jean, C. Tellez, M. Bar-Eli, R. Frade, Inhibition of tumorigenicity and metastasis of human melanoma cells by anti-cathepsin L single chain variable fragment. Cancer Res. 64 (2004) 146–151.

[41] R.E. Burden, P. Snoddy, C.A. Jefferies, B. Walker, C.J. Scott, Inhibition of cathepsin L-like proteases by cathepsin V propeptide. Biol. Chem. 388 (2007) 541–545.

[42] R.E. Burden, P. Snoddy, R.J. Buick, J.A. Johnston, B. Walker, C.J. Scott, Recombinant cathepsin S propeptide attenuates cell invasion by inhibition of cathepsin L-like proteases in tumor microenvironment. Mol. Cancer Ther. 7 (2008) 538–547.

[43] A. Rebbaa, F. Chu, T. Sudha, C. Gallati, U. Dier, E. Dyskin, M. Yalcin, C. Bianchini, O. Shaker, S.A. Mousa, The anti-angiogenic activity of NSITC, a specific cathepsin L inhibitor. Anticancer Res. 29 (2009) 4473–4481.

[44] C.J. Scott, C.C. Taggart, Biologic protease inhibitors as novel therapeutic agents, Biochimie, in press.

[45] C. Le Gall, A. Bellahcene, E. Bonnelye, J.A. Gasser, V. Castronovo, J. Green, J. Zimmermann, P. Clezardin, A cathepsin K inhibitor reduces breast cancer induced osteolysis and skeletal tumor burden. Cancer Res. 67 (2007) 9894–9902.

[46] C. Le Gall, E. Bonnelye, P. Clezardin, Cathepsin K inhibitors as treatment of bone metastasis. Curr. Opin. Support Palliat. Care 2 (2008) 218–222.

[47] E.M. Lewiecki, Odanacatib, a cathepsin K inhibitor for the treatment of osteoporosis and other skeletal disorders associated with excessive bone remodeling. IDrugs 12 (2009) 799–809.

[48] D. Bromme, F. Lecaille, Cathepsin K inhibitors for osteoporosis and potential off-target effects. Expert Opin. Investig. Drugs 18 (2009) 585–600.